I. INTRODUCTION

This report examines the relationship between the mass of objects of similar three-dimensional geometry with respect to its angular acceleration. A rotary motion sensor installed at the base of the apparatus will record angular position data as the disk, with various hollow cylindrical masses on top, spins due to the tension on the attached string (Figure 1). The string connects the disk with the hanging mass through the 3-step pully and the super pully. Its tension force is the result of the force of gravity enacting down upon the hanging mass. The objective of this experiment is to experimentally determine the moment of inertia (I) of the various hollow cylindrical masses.

The equations for rotational motion are analogous to translational motion with the replacement of mass, position, velocity and acceleration with the I, angular position, angular velocity and angular acceleration, respectively. The equations for torque, angular momentum and rotational kinetic energy, which are analogous to force, momentum and kinetic energy, respectively, are expressed in Figure 2. The theoretical I for a hollow cylinder at its center of mass is expressed in Figure 3.

II. PROCEDURE

The experiment apparatus consists of the Pasco Scientific Complete Rotational System set along with a computer which runs the Pasco Capstone Software. Initially, the mass and dimensions of the aluminum disk, the mass hanger, the hollow

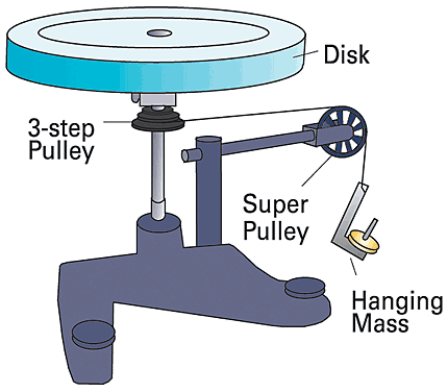

Figure 1: *The experiment apparatus whereby the gravitational force exerted on the hanging mass causes the unwinding of the string attached to the disk. This generates a torque which produces rotational motion from the disk. (Pasco 2017)*

[1] $\boldsymbol{\tau = I\alpha = RFsin\theta}$

[2] $\boldsymbol{L = Iw}$

[3] $\boldsymbol{K = \frac{1}{2}Iw^2}$

Figure 2: *Equations for torque [1], angular momentum [2], and rotational kinetic energy. τ is torque, I is the moment of inertia, α is the angular acceleration, R is the length of the moment arm, F is the perpendicular force, θ is the angle between the force vector and the moment arm, L is the angular momentum, w is the angular frequency, and K is the rotational kinetic energy.*

[1] $\boldsymbol{I_{CM} = \frac{1}{2}M(R_1{}^2 + R_2{}^2)}$

[2] $\boldsymbol{I_{CM} = \frac{1}{2}MR_2{}^2}$

Figure 3: *Equations of I of hollow cylinder [1] and disk [2]. I_{CM} is the moment of inertia for a hollow cylinder at its centre of mass, M is the mass of the hollow cylinder, R_1 is the internal radius, and R_2 is the external radius.*

cylindrical masses, and the washer rings to be attached to the mass hanger were measured (Table I) using a measuring scale (±0.1 g) and a digital Vernier Caliper (±0.01 mm). To set up the apparatus, a thread is attached to the 3-step pully and secured to the hanging mass on the other end by tying knots. The length of the thread is cut to be less than the distance between the apparatus and the ground to ease the identification of the accelerated range in the angle-time graph. The span of the thread is rested on the super pully. By turning the aluminum disk counterclockwise, the thread is winded until the hanging mass reaches the super pully. Three different hollow cylindrical masses were placed on top of the aluminum disk for experimentation with three different hanging masses. In addition to these nine runs, three runs were conducted without any mass on top of the aluminum disk to determine its I. The aluminum disk is first leveled using a spirit level. Upon recording using the rotary motion sensor, the external force of equal magnitude against gravity on hanging mass is released to allow the thread to unwind. After each run, the apparatus is re-winded. The collection frequency set to 50 Hz.

	Mass (±0.1 g)	Outer Diameter (±0.01 mm)	Thickness (±0.01 mm)
Aluminum Disk	120.1	95.19	N/A
Mass Hanger	25.3	N/A	N/A
3-Step Pully	6.8	49.76	N/A
Hollow Cylinder #1 (Bronze)	453.7	76.22	10.18
Hollow Cylinder #2 (Black)	472.5	76.55	11.53
Hollow Cylinder #2 (Silver)	125.6	76.00	10.05
Washer #1	16.7	N/A	N/A
Washer #2	16.8	N/A	N/A

Table 1: *Mass and length measurements of various components used in the experiment.*

Using the Capstone Software, the angle of the aluminum disk as it rotates is graphed as a function of time and its accelerated range is fitted to a quadratic function for each run. The format of this function is in the form of $At^2 + Bt + C$, where A, B, and C are constants. Using the equation of $\theta_f = \theta_i + w_i t + \frac{1}{2}\alpha t^2$, where θ_f is the final angle, θ_i is the initial angle, w_i is the initial angular frequency, α is the angular acceleration, and t is time, the angular acceleration of the aluminum disk

can be calculated by equating $A = \frac{1}{2}\alpha$, where $\alpha = 2A$. For example, for Run #1, where the aluminum disk, without any mass on top, was angularly accelerated by the hanging mass, the value of A from the quadratic fit of its angle-time graph was 18.70±0.03. Thus, its angular acceleration is 37.40±0.06 rads^{-2}.

In two additional runs, the silver and bronze hollow cylinders were dropped onto the rotating aluminum disk to determine and compare the possible conservation of angular momentum and rotational energy before and after the collision. The angle-time graph during this process is shown in Figure 4.

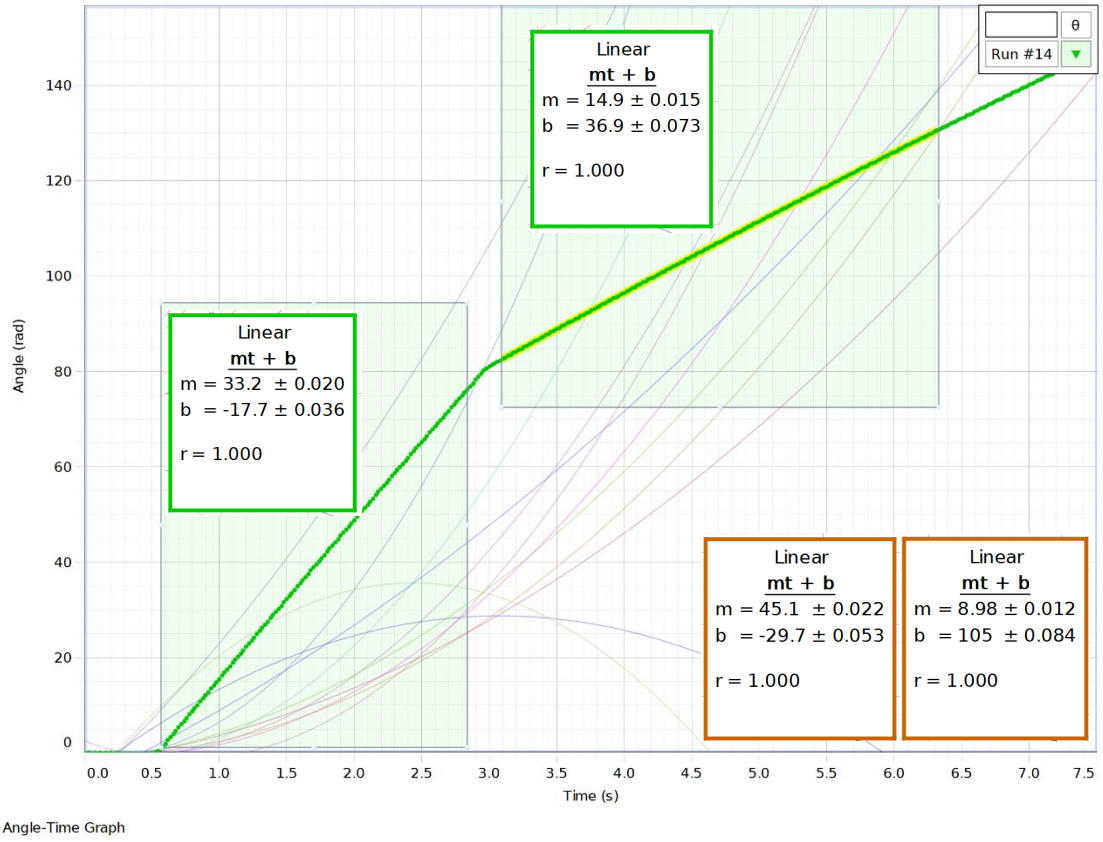

Figure 4: *Angle-time graph of the rotation of the aluminum disk before and after the dropping of the silver hollow cylinder onto it. The two linear fits within the green boxes corresponds to the two linear lines. The two brown boxes identify a similar angle-time graph, which is not shown, after the dropping of the bronze hollow cylinder.*

III. RESULTS AND DISCUSSION

To find the I of the aluminum disk along with any hollow cylinders on top, one can use the equation $\frac{1}{\alpha} = \left(\frac{I}{gR}\right)\left(\frac{1}{m}\right) + \frac{R}{g}$, where α is the angular acceleration, g is the gravitational force, I is the

moment of inertia, and R is the radius of the 3-step pully (the distance of the applied force to the center of the aluminum d). This equation is derived through the analysis model of the acceleration of falling mass attached to a rotating disc which uses a combination of the equations in Figure 2. The equation is also in the form of $y = mx + b$ which means $\frac{I}{gR}$ (slope) can be found by plotting $\frac{1}{\alpha}$ (x-value) with respect to $\frac{1}{m}$ (y-value). Since g and R are known, I can be solved (Figure 5). The initial I of the hollow cylinders must be subtracted by the I of the aluminum disk to attain their true value since both masses experienced the torque of from the thread during experimentation. As a result, the I of the aluminum disk, bronze, black, and silver hollow cylinders are 2.98±0.01E-4, 1.12±0.01E-3, 1.15±0.01E-3, and 3.22±0.01E-4 kgm^2, respectively. The uncertainties are calculated through percentage uncertainties of the slope, g, and R. The value of g in Toronto is 9.806 78±0.000 01 ms^{-2} (Wolfram 2017).

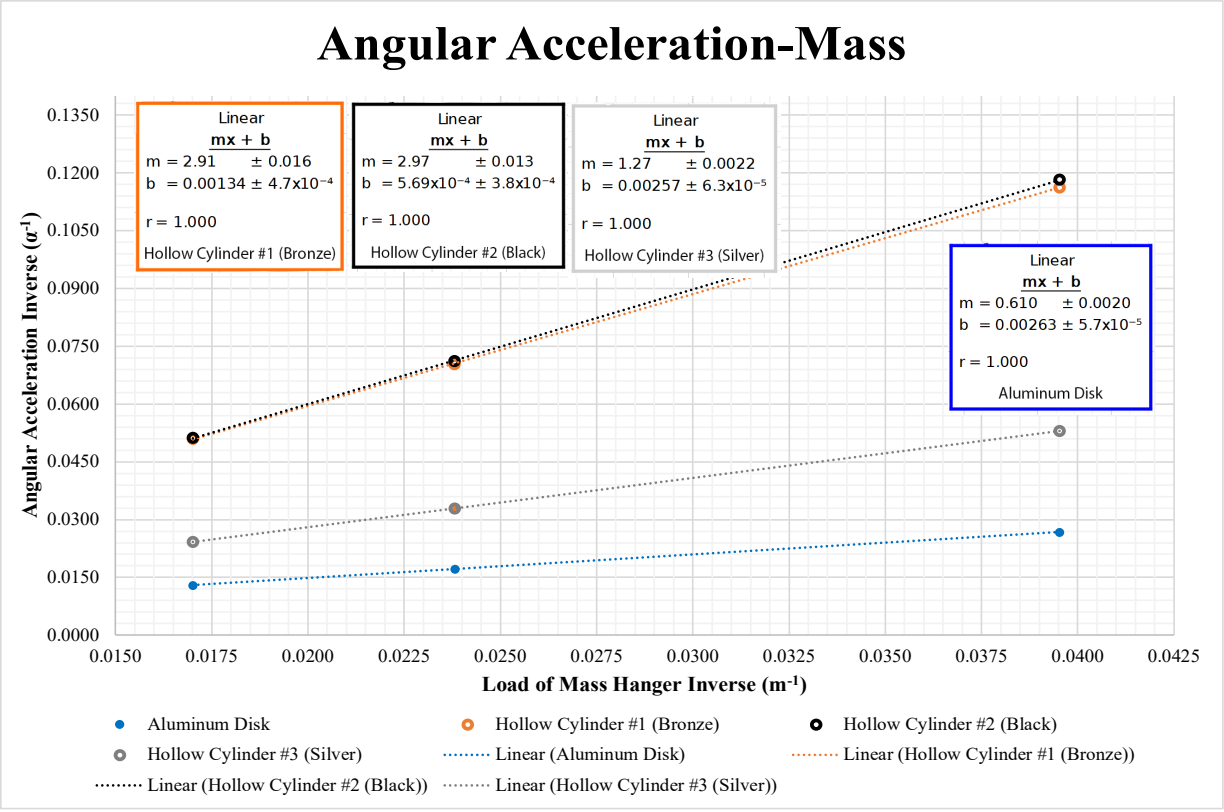

Figure 5: *Angular acceleration-mass graph created by graphing $\frac{1}{m}$ with respect to $\frac{1}{\alpha}$. The data points of different colours represent different loads on the aluminum disk. The dashed lines are linear fit lines corresponding to the data points of identical colour. The error bars for both axis, calculated through percentage error, is too insignificant to be identified.*

By using the equation in Figure 3, the theoretical values of I of the aluminum disk, bronze, black, and silver hollow cylinders are 1.36±0.01E-4, 5.06±0.01E-4, 5.15±0.01E-4, and 1.40±0.01E-4 kgm^2, respectively. The uncertainties are calculated through percentage uncertainties of the mass, outer diameter, and the thickness. The outer radius is found by halving the outer diameter while the inner radius is found by subtracting the outer radius by the thickness. These theoretical values of I are comparable to the experimentally determined values by about a factor of two and are outside of uncertainty. The errors of the data collection and processing which contributed to such inaccuracies will be discussed later.

Since the derivative of angular displacement (θ) with respect to time is the angular frequency (ω), the slope (m) of the graph in Figure 4 represents ω. As a result, the angular momenta and rotational energies of the silver and bronze hollow cylinder-aluminum disk systems can be found using the equations in Figure 2 (Table II). The I of the aluminum disk is used to calculate L_i and K_i while the sum of the I of the aluminum disk and the hollow cylinder is used to calculate L_f and K_f. The uncertainties are calculated through percentage uncertainties of I and ω. While L_i and L_f for both cylinders do not agree to within uncertainty, the differences are much smaller when compared to K_i and K_f. Theoretically, angular momentum is conserved due to the absence of external torque on the system during collision, while rotational energy is not conserved since the collision is inelastic in nature.

HC	I (E-4kgm^2)	w_i ($rads^{-1}$)	w_f ($rads^{-1}$)	L_i (E-3 kgm^2s^{-1})	L_f(E-3 kgm^2s^{-1})	K_i (E-2J)	K_f (E-2J)
Silver	1.40±0.01	33.2±0.0	14.9±0.0	4.52±0.01	4.11±0.01	7.50±0.01	3.06±0.01
Bronze	5.06±0.01	45.1±0.0	8.98±0.01	6.13±0.01	5.77±0.01	13.8±0.1	2.59±0.01

Table II: *Angular momentum and rotational energy comparison before and after the separate inelastic collisions of the two hollow cylinders (HC) on the rotating aluminum disk. The subscripts i and f means initial and final, respectively.*

The uncertainties involved in this experiment consists of the measurement uncertainty associated with the rotary motion sensor (±0.002 rad), and all mass (±0.1 g) and length (±0.01 mm) measurements. It also consists of the estimation by inspection of the placement of the hollow cylinders on the center of the aluminum disk along with the negligence of the mass of the 3-step pully and the

thread and the I of the super pully. The three statistical uncertainties consist of the quadratic fitting of the angle-time graph for each run and the linear fitting of both the collision angle-time graph the acceleration-mass graph. The dominant uncertainty is likely associated with the random error in the placement of the hollow cylinders since any deviation from the exact center will alter the values of I.

IV. CONCLUSION

The experiment has succeeded in identifying a negative linear correlation between the mass of objects of similar 3D geometry with respect to its angular acceleration. The objective of the experiment has been met by experimentally determining I of various masses. This consists of the aluminum disk, bronze, black, and silver hollow cylinders which their I corresponds to 2.98±0.01E-4, 1.12±0.01E-3, 1.15±0.01E-3, and 3.22±0.01E-4 kgm^2, respectively. The moderate deviation from the theoretical values of 1.36±0.01E-4, 5.06±0.01E-4, 5.15±0.01E-4, and 1.40±0.01E-4 kgm^2, respectively, is blamed primarily on the random error of the placement of the cylindrical masses on the aluminum disk.

The method to experimentally determine I involved collecting angular displacement data of the aluminum disk due to the torque exerted by the hanging mass. The data for each run is then graphed and quadratically fitted to determine the angular acceleration. The inverses of the mass of the hanging mass and the angular acceleration for each cylindrical mass are then graphed and linearly fitted. I is the product of the slope of the graph's linear fit, the gravitational force, and the radius of the 3-step pully.

While more trials and more loads on both the aluminum disk and the mass hanger can be explored to improve the experiment's accuracy, the use of markings and securing the cylindrical masses on the aluminum disk can likely produce significantly more accurate I values.

The experiment can be extended by allowing the aluminum disk to continue its rotation after the unwinding of the thread until it stops due to the loss of mechanical energy from primarily the kinetic friction of the rotation axle. Different masses can be placed on top of the aluminum disk to determine the coefficient of kinetic friction of the axle.

References

Pasco. (2017). Complete Rotational System [Digital image]. Retrieved November 8, 2017, from https://www.pasco.com/prodCatalog/ME/ME-8950_complete-rotational-system/

Wolfram. (2017). Gravitational field strength for Toronto, Canada. Retrieved November 8, 2017, from https://www.wolframalpha.com/input/?i=gravity%2Btoronto